A conceptual study on the prediction of destress blasting efficiency using geostatistical approaches

Tawanda Zvarivadza
Luleå University of Technology, Luleå, Sweden

ABSTRACT: As underground mines go deeper, it is of utmost importance to manage increased stresses to minimise occurrences of rockbursts. Rockbursts have several documented devastating economic, social and safety consequences such as fatalities, loss of mine assets or production sections, social uproar, force majeure etc. Among several approaches which can be adopted to manage rockbursts is the practice of destress blasting. It is necessary to evaluate the efficiency of any adopted destress blasting design. This can be done through the measurement of physical parameters such as changes in deformation, local seismic magnitude, stress; fracturing intensity etc. at different locations where destress blasting has been implemented. This entails physical exposure of workers to mining excavations, increasing their exposure to harm when safety fails. This paper presents a conceptual study on geostatistical approaches which can be utilized to estimate unmeasured locations using measured locations, thereby reducing the mining personnel's exposure to harm.

Keywords: Deep mining, Rockburst, Destress blasting, Geostatistics, Semi-variogram modelling, Cross-validation.

1 INTRODUCTION

Deep hard rock mining faces the challenges of rockbursts due to increasing stresses and deformations at depths. When the accumulated stress is not properly managed, the resultant rockbursts can lead to severe consequences such as fatalities, loss of expensive equipment, loss of mine production sections, social uproar, and force majeure among many other consequences.

Among the alternatives to manage the high stresses and deformations is the practice of destress blasting. Destress blasting aims to move peak stress from the immediate vicinity of the mining drift further into the rock mass (Roux et al. 1958).

To come up with a suitable destress blast design, accurate information on the rock mass properties, excavation geometry, stress regime, blast hole dimensions and explosives characteristics is needed. To assess the efficiency of destress blasting, different approaches can be used, these include, numerical simulation, fracture frequency monitoring ahead of the mining face (using a borehole camera, ground penetrating radar or physical assessment of the mining face drill core) before and

after destress blasting, deformation monitoring using laser scanning among many other approaches. Figure 1 illustrates fracture frequency measurement using borehole periscope (a) and physical assessment of drill core (b). c represents a scale which can be used to assess rockburst potential based on fracture frequency measurement.

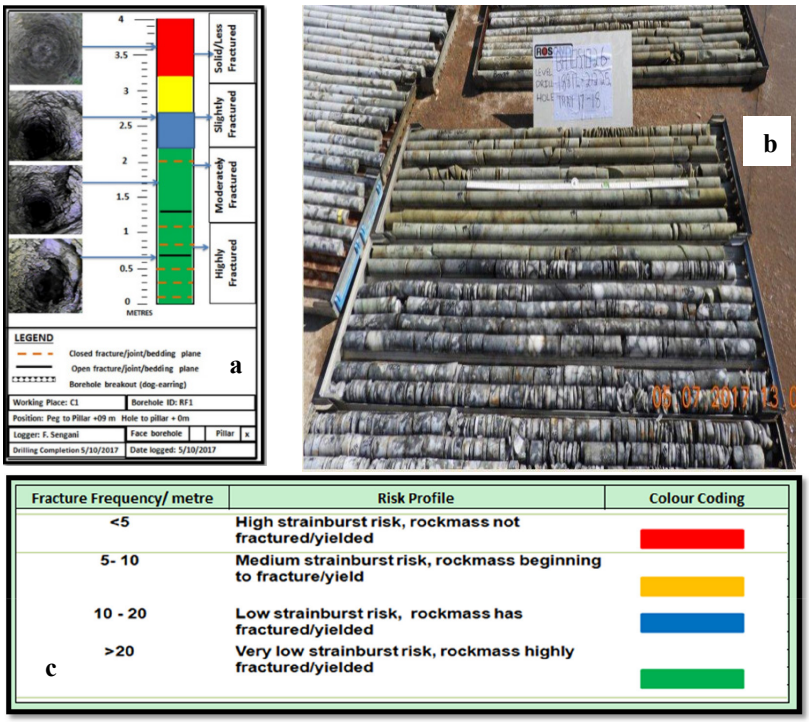

Figure 1. a Rock fracturing observation for a mining pillar (pillar face to pillar core (centre)) using a borehole camera (Sengani, 2020). b Rock fracturing ahead of a mining face as observed from mine drill core after destress blasting (Sengani & Zvarivadza, 2018). c Fracture frequency interpretation in relation to rockburst potential (Sengani & Zvarivadza, 2017).

Given a set of geological and geotechnical conditions of the mine, geostatistical approaches can be used to predict the performance of destress blasting at different sections of the mine, mined or not mined. This study makes use of the geostatistical approaches of Semi-variogram modelling and Kriging to predict the efficiency of destress blasting for deep-level mining. The confidence in the results is given with a level of confidence of 95%. The concept of Semi-variogram modelling is credited for its ability to capture geological variability in the rockmass, with the determined standard deviation enabling rock engineers to assess the risk associated with a chosen destress blast design.

2 GEOSTATISTICAL APPROACHES TO PREDICT DESTRESS BLASTING EFFICIENCY

Several physical mining parameters can be separately evaluated using geostatistical approaches to estimate the value of that parameter at an unmeasured particular location of the mine, using historical observations. Some of the parameters which can be geostatistically analysed to evaluate destress blasting efficiency include deformation changes, local seismic magnitude changes, stress changes, and fracturing intensity among others. Collection of these parameters in an underground mine entails visiting the mining locations and performing physical measurements (laser scanning for deformation monitoring, installation of seismic monitoring devices, stress measurement devices, ground penetrating radar scanning or borehole camera measurement for fracture intensity monitoring.

It can be seen that evaluation of the destress blasting efficiency entails physical encounters with the mining operations and can be costly. The need to make the aforementioned measurements increases the number of encounters and amount of time workers are exposed to the underground

mining faces, increasing the risk of mining personnel harm in the event of unanticipated safety failures. While there are several physical parameters which can be evaluated to analyse destress blasting efficiency, this paper focuses on the use of fracture frequency analysis approach, as postulated by Sengani and Zvarivadza (2017), to evaluate destress blasting efficiency from a geostatistical perspective. The use of fracture frequency analysis to evaluate destress blasting efficiency is credited for being practical and tethered in reality, that is, the observed results are based on what is actually happening in the rockmass, unlike other approaches such as numerical modelling which need several assumptions to be considered since the model cannot capture all the factors which influence rockmass behaviour. This practical, empirical approach inherently accounts for the most likely rockmass behaviour at a particular location based on historical observations. Despite the mentioned concerns of workers' safety, some locations to be measures for destress blasting efficiency evaluation are simply not available due to several operational reasons such as scheduled blasting, scheduled charging, charged end, closed due to rock falls, entrance not passable due to other obstacles such as water, unavailability of transport to visit the mining end among many others.

2.1 Semi-variogram analysis

Semi-variogram analysis makes use of measured or known data of a particular parameter to estimate the value of that particular parameter at an unmeasured location. This approach has been used in many different fields of research, be it agriculture, pollution analysis, mining resources estimation, water quality distribution, fisheries, and forestry management among others. The spatial correlation of the parameter at the unmeasured location with other measured locations enables the estimation of the parameter as the unmeasured location with a great degree of confidence. This saves time, and resources and puts a buffer between workers and harm in the case of deep underground mining.

2.1.1 Experimental Semi-variogram

Data on the physical mining parameter to be analysed can be gathered based on the actual measurements which have been done on the mine and updated continuously. These actual measurement data can be represented in an Experimental Semi-variogram (See Figure 2), giving the semi-variance between pairs of samples at certain distances. Each point in the Experimental Semi-variogram represents several pairs of samples with the same distance between them. Equation 1 is the formula for determining the Experimental Semi-variogram (γ_h*)

$$\gamma_h^* = \frac{1}{2N_h}\sum(f_i - f_j)^2 \qquad (1)$$

Where N_h is the number of samples at distance h. fi and fj represent the fracture frequency at locations i and j respectively.

2.1.2 Model Semi-variogram

Once the data on the Experimental Semi-variogram is available, it can then be used to estimate the value of the assessed parameter at the unmeasured location. The most challenging part of geostatistics is to fit the most appropriate geostatistical model to the experimental data in order to have more accurate estimations. Fitting of the most appropriate model to the experimental data entails several iterations where the model parameters (Total sill (C_T), Nugget effect (C_0) and Range (a) are continuously adjusted until the best possible model fit is attained. Fitting a geostatistical model to the experimental data is more of an art than a science, yet the fitted model and its parameters directly affect the determination of confidence intervals of our estimates. In this study, three Model Semi-variograms were fitted on the Experimental Semi-variogram, with the model parameters of each Model Semi-variogram being adjusted several times to achieve the most reasonable best fit. The Model Semi-variograms are presented in Table 1. Figure 2 shows the Experimental Semi-variogram with the fitted Model Semi-variograms.

Table 1. Model Semi-variograms fitted to the Experimental Semi-variogram.

Spherical Model Semi-variogram	**Exponential Model Semi-variogram**	**Gaussian Model Semi-variogram**
$\gamma(0) = 0$	$\gamma(0) = 0$	$\gamma(0) = 0$
$\gamma(h) = C_0 + C_1\left(\frac{3h}{2a} - \frac{1h^3}{2a^3}\right)$	$\gamma(h) = C_0 + C_1\left[1 - \exp\left(-\frac{h}{a}\right)\right]$	$\gamma(h) = C_0 + C_1\left[1 - \exp\left(-\frac{h^2}{a^2}\right)\right]$
for $0 < h < a$	for $h > 0$	for $h > 0$
$\gamma(0) = C_0 + C_1$ for $h > a$		
C_0: 1.6 C_T: 3.6 C_1: 2 a: 141	C_0: 1.4 C_T: 4.5 C_1: 3.1 a: 115	C_0: 1.8 C_T: 5 C_1 3.2 a: 150

Note: C_0 is the nugget effect, random variation within the sampled data; C_T is the total sill, maximum variance within the sampled data; C_1 is the Spherical component, that is C_T - C_0; a is the range, that is the distance between samples beyond which the samples are no longer related.

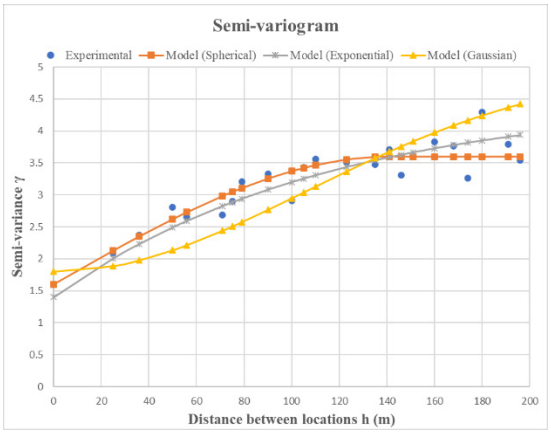

Figure 2. Experimental Semi-variogram with fitted Model Semi-variograms.

2.1.3 Model Semi-variogram choice and Cross-validation

From the Experimental Semi-variogram (Figure 2), it can be noted that the maximum possible Sill of the experimental data is 4.29. Attempting to fit a Model Semi-variogram using this sill will leave out several experimental data, resulting in an erroneous model. From the artful fitting of the Model Semi-variogram, it can be seen that adopting a sill of 3.6 will result in a Spherical model Semi-variogram which suitably fits the Experimental Semi-variogram. As can be noted from Figure 2, the Gaussian Model Semi-variogram does not fit the experimental data well, despite adjusting the sill to 5, a value above the maximum sill noted in the Experimental Semi-variogram. The Exponential model Semi-variogram appears to fit the experimental data but it is based on a sill fit of 4.5, which excludes most of the Experimental data.

A Cross-validation exercise can be done on the different models, utilizing different model parameter values to ascertain if a chosen model and its parameter values would give accurate results when estimating the value of an unmeasured location. In the Cross-validation exercise, a set of known readings following a particular uniform layout (see Figure 3) are used to test the models. In this

layout, all the values are known, only that other values are assumed to be unknown (L5, L6, L7) so that they are estimated using the models.

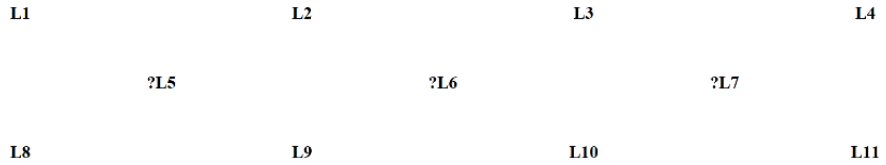

Figure 3. Uniform layout of known samples used for the Model Semi-variogram Cross-validation exercise.

A Cross-validation statistic is calculated for each unknown point (assumed to be unknown) in order to assess the model. The Cross-validation statistic (Z) together with its mean (μ_Z) and variance (σ^2_Z) are determined using the following Equations.

$$Z = \frac{T - T^*}{\sigma_\epsilon} \qquad \mu_Z = \frac{1}{n}\sum Z_i \qquad \sigma_Z^2 = \frac{1}{n}\sum (Z_i)^2$$

Where: T is the true value; T* is the estimated value, calculated using Equation 2.

$$T^* = w_1 f_1 + w_2 f_2 + w_3 f_3 + \cdots w_n f_n \qquad (2)$$

A model which accurately captures the underlying variability within the Experimental Semi-variogram data should ideally yield a Cross-validation statistic mean (μ_Z) of zero and a Cross-validation statistic standard deviation (σ_Z) of 1. This is because the variable Z, in this format, follows a normal distribution regardless of the distribution of T*.

f is the measured fracture frequency in this case, and w is the weight of the sample used in the estimation. The sum of the weights is always equal to 1. The weight of the samples can be determined using the standard Inverse Distance Estimation Technique (IDET). However, the IDET method has several disadvantages, which makes it unable to produce optimum weights for the samples. Some of the disadvantages are that we are never certain which distance function to use, we are not sure how many samples should be included in the estimation of a point, we do not know how far we can go, in terms of distances, to include samples in the estimation of a point, our confidence in the estimated value is questionable since we cannot determine the confidence interval of our estimate among others. These shortcomings are overcome using the Ordinary Kriging Technique as discussed in section 2.1.4.

σ_ϵ is the standard deviation of the estimation errors, when using 4 known points to estimate an unknown point, σ_ϵ is given as shown in Equation 3. The equation can be expanded using its obvious pattern to use as many as geostatistically possible known samples in the estimation procedure. These types of calculations are normally carried out using geostatistics software as the number of samples to be analysed, having been collected over a very long period of time, can easily become so many, the same applies with Ordinary Kriging (OK) calculations.

$$\sigma_\epsilon^2 = 2w_1\gamma(d_1) + 2w_2\gamma(d_2) + 2w_3\gamma(d_3) + 2w_4\gamma(d_4) - \begin{Bmatrix} w_1w_1\gamma(h_{11}) + w_1w_2\gamma(h_{12}) + w_1w_3\gamma(h_{13}) + w_1w_4\gamma(h_{14}) \\ +w_2w_1\gamma(h_{21}) + w_2w_2\gamma(h_{22}) + w_2w_3\gamma(h_{23}) + w_2w_4\gamma(h_{24}) \\ +w_3w_1\gamma(h_{31}) + w_3w_2\gamma(h_{32}) + w_3w_3\gamma(h_{33}) + w_3w_4\gamma(h_{34}) \\ +w_4w_1\gamma(h_{41}) + w_4w_2\gamma(h_{42}) + w_4w_3\gamma(h_{43}) + w_4w_4\gamma(h_{44}) \end{Bmatrix} - 0 \qquad (3)$$

Where: d is the distance between a known sample and the location to be estimated. h is the distance between known samples.

2.1.4 Ordinary Kriging

Ordinary Kriging (OK) is credited for being the Best Linear Unbiased Estimator (BLUE) as it gives the best estimate (Equation 2) of the value at an unmeasured location, at the narrowest confidence

interval (Equation 5) and smallest estimation error variance (σ_{OK}^2) (Equation 4). The OK procedure makes use of the Lagrangian multiplier (λ) to develop a system of equations (see below) which can be solved to get the optimum weights, which can be used in the estimation of the unknown value. OK procedure addresses most of the challenges associated with IDET. In geostatistical estimation, we are more interested in the level of confidence we have in our estimate, than just having the estimate itself. We can now determine the 95% confidence interval of the True value (T) by determining the lower limit and upper limit of the True value using Equation 5. Note that the narrower the confidence interval, the more accurate our estimate is. The level of accuracy is enhanced by choosing the best model using Cross-validation and using optimum weights determined from OK.

$$
\begin{aligned}
&w_1\gamma(h_{11}) + w_2\gamma(h_{12}) + w_3\gamma(h_{13}) + w_4\gamma(h_{14}) + \lambda = \gamma(d_1)\\
&w_1\gamma(h_{21}) + w_2\gamma(h_{22}) + w_3\gamma(h_{23}) + w_4\gamma(h_{24}) + \lambda = \gamma(d_2)\\
&w_1\gamma(h_{31}) + w_2\gamma(h_{32}) + w_3\gamma(h_{33}) + w_4\gamma(h_{34}) + \lambda = \gamma(d_3)\\
&w_1\gamma(h_{41}) + w_2\gamma(h_{42}) + w_3\gamma(h_{43}) + w_4\gamma(h_{44}) + \lambda = \gamma(d_4)\\
&w_1 + w_2 + w_3 + w_4 + 0 = 1
\end{aligned}
$$

$$\sigma_{OK}^2 = w_1\gamma(d_1) + w_2\gamma(d_2) + w_3\gamma(d_3) + w_4\gamma(d_4) + \lambda \quad (4)$$

$$T = T^* \pm 1.9600 \times \sigma_{OK} \quad (5)$$

3 CONCLUSIONS

Destress blasting plays a pivotal role in stress management in deep underground mines. In an endeavour to evaluate destress blasting efficiency, physical parameters such as deformation changes, local seismic magnitude changes, stress changes, and fracturing intensity among others are collected from different locations where destress blasting has been implemented. This leads to increased exposure of mining personnel to mining excavations, increasing the chances of harm in the event of safety failure. This paper presents a conceptual study on the use of geostatistical methods to accurately estimate the destress blasting efficiency at some of these locations, without physically visiting them to take measurements. This can be done with a high degree of accuracy using geostatistical spatial relations of locations as captured by a geostatistical model fitted on the actual experimental data of measured locations, lending credence to this approach as these practical observations are tethered in reality and to some extent account for several factors which affect rock behaviour, which may be difficult to account for using numerical modelling. The confidence interval of each estimate at an unmeasured location can be determined, realistically, to 95% accuracy using optimised sample weights determined from OK and a Semi-variogram model verified using the Cross-validation exercise.

REFERENCES

Roux, A.J.A., Leeman, .ER. & Denkhaus, H.G. 1958. De-stressing: a means of ameliorating rockburst conditions: Part I: The concept of de-stressing and the results obtained from its application, by AJA Roux, ER Leeman and HG Denkhaus, published in the Journal, October, 1957: author's reply to discussion. *Journal of the Southern African Institute of Mining and Metallurgy*, *59*(1), pp.66-68.

Sengani, F. & Zvarivadza, T. 2017. Review of pre-conditioning practice in mechanized deep to ultra-deep level gold mining: 26th International Symposium on Mine Planning and Equipment Selection (MPES2017). 29–31 August 2017, Luleå, Sweden.

Sengani, F. & Zvarivadza, T. 2018. March. Borehole periscope observations of rock fracturing ahead of the preconditioned mining faces in a deep level gold mine. In *ISRM 1st International Conference on Advances in Rock Mechanics-TuniRock 2018*. OnePetro.

Sengani, F. 2020. The use of ground Penetrating Radar to distinguish between seismic and non-seismic hazards in hard rock mining. *Tunnelling and Underground Space Technology*, *103*, 103470. https://doi.org/10.1016/j.tust.2020.103470.